Journal Name

Dynamic Article Links ►

Cite this: DOI: 10.1039/c0xx00000x

www.rsc.org/xxxxxx

ARTICLE TYPE

New Directions for Hydrogen Storage: Sulphur Destabilized Sodium Aluminium Hydride

Drew A. Sheppard*[a], Lars H. Jepsen[b], Torben R. Jensen[b], Mark Paskevicius[a] and Craig E. Buckley[a]

Received (in XXX, XXX) Xth XXXXXXXXX 20XX, Accepted Xth XXXXXXXXX 20XX

DOI: 10.1039/b000000x

Aluminium sulphide (Al_2S_3) is predicted to effectively destabilize sodium aluminium hydride ($NaAlH_4$) in a single-step endothermic hydrogen release reaction. The experimental results show unexpectedly complex desorption processes and a range of new sulphur containing hydrogen storage materials have been observed. The $NaAlH_4$-Al_2S_3 system releases a total of 4.9 wt.% of H_2 that begins below 100 °C without the need for a catalyst. Characterization via Temperature Programmed Desorption, *in-situ* Synchrotron Powder X-ray Diffraction, *ex-situ* X-ray Diffraction, *ex-situ* Fourier Transform Infrared Spectroscopy and hydrogen sorption measurements reveal complex decomposition processes that involve multiple new sulphur-containing hydride compounds. The system shows partial H_2 reversibility, without the need for a catalyst, with a stable H_2 capacity of ~1.6 wt.% over 15 cycles in the temperature range of 200 °C to 300 °C. This absorption capacity is limited by the need for high H_2 pressures (> 280 bar) to drive the absorption process at the high temperatures required for reasonable absorption kinetics. The large number of new phases discovered in this system suggests that destabilization of complex hydrides with metal sulphides is a novel but unexplored research avenue for hydrogen storage materials.

Introduction

Hydrogen is considered to be a key future energy carrier [1] but its safe, compact and efficient storage are one of the key barriers to its widespread use. Hydrogen can be stored in the solid state using complex metal hydrides where the hydrogen is covalently bonded in complex anions such as AlH_4^{-1}, AlH_6^{-3}, BH_4^{-1} and NH_2^- [1].

Of the class of complex metal hydrides known as complex Aluminium hydrides, or alanates, $NaAlH_4$ is the most studied [2-4] and has a theoretical hydrogen storage capacity of 7.5 wt.% that is released via three reactions:

$3NaAlH_4 \rightarrow Na_3AlH_6 + 2Al + 3H_2$ Reaction 1

$Na_3AlH_6 \rightarrow 3NaH + Al + 3/2H_2$ Reaction 2

$NaH \rightarrow Na + 1/2H_2$ Reaction 3

Reaction 1 and 2 can occur below 150 °C (with the aid of a catalyst) but Reaction 3 requires more than 400 °C and is not of practical use. As a result, not all of the hydrogen contained within $NaAlH_4$ can be readily released and the useable hydrogen capacity is limited to the first two steps (5.6 wt.% H_2). To make Reaction 1 and 2 reversible requires the addition of a catalytic phase [3, 5] that aids in the distortion of Al-H bonds at the $NaAlH_4$ interface.[5] For example, the use of $TiCl_3$ as a catalyst also results in an irreversible reaction with the $NaAlH_4$ in a metathesis reaction:[6]

$3NaAlH_4 + TiCl_3 \rightarrow 3NaCl + xAl + Al_{3-x}Ti + 6H_2$ Reaction 4

The end result is that the practical capacity of $NaAlH_4$ is typically reduced to the range of 3.0 – 4.5 wt.%.[7, 8]

The major drawbacks of alanates are: (1) that they release hydrogen in multiple desorption events (a disadvantage in engineering applications); (2) that not all the hydrogen can easily be released and (3) that the addition of catalysts reduces the practical hydrogen capacity.

A potential clue to an alternative approach to improve the hydrogen storage properties of complex metal hydrides is in the reaction of $TiCl_3$ with $NaAlH_4$ (Reaction 4). Though the reaction is exothermic and irreversible, when $TiCl_3$ is added in stoichiometric quantities, it does release all of the hydrogen in $NaAlH_4$. Finding a similar reaction that releases all of the hydrogen in an endothermic process would mean that the hydrogen release is potentially reversible.

Alapati *et al.*[9] used Density Functional Theory to screen for reversible hydrogen storage reactions based on all possible known combinations of 13 selected light elements and first row transition metals. In a similar approach we have used the thermodynamic data [10, 11] and HSC software [12] to explore the enthalpy of reaction between $NaAlH_4$ and a range of metal oxides, metal halides and metal sulphides in an attempt to find a suitable reaction that releases all of the hydrogen in a single endothermic step while maintaining high hydrogen content. These calculations suggested that $NaAlH_4$ mixed with Al_2S_3 could achieve the desired effect as shown in Reaction 5 (Figure 1):

$6NaAlH_4 + Al_2S_3 \rightarrow 3Na_2S + 8Al + 12H_2$ Reaction 5

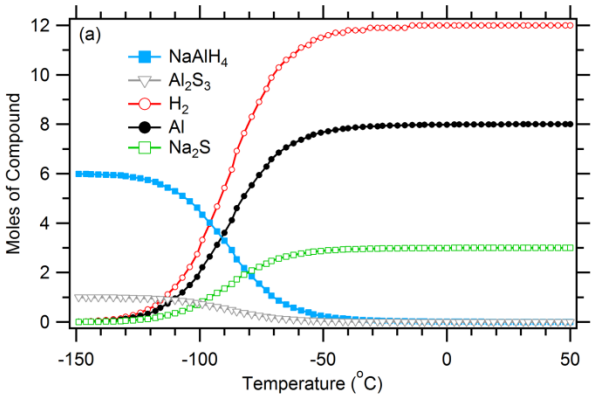

Fig 1. Predicted decomposition of $NaAlH_4$ mixed with Al_2S_3 (6 to 1 mole ratio) as a function of temperature.

Reaction 5 has a theoretical H_2 capacity of 5.1 wt.% (1 bar equilibrium temperature (T_{eq}) = -109 °C) compared to a theoretical value of 5.6 wt.% for pure $NaAlH_4$ (first two steps: 1 bar T_{eq} = 33 °C and 105 °C). [10] Though the capacity is slightly lowered, all of the hydrogen release is predicted to occur in a single step; a significant advantage for engineering applications. The addition of Al_2S_3 also results in an increased volumetric density of hydrogen (74 kg of H_2/m^3) compared to pure $NaAlH_4$ (71 kg of H_2/m^3). While the weight of a hydrogen tank for mobile applications is important, the volume the tank takes up within a passenger vehicle is also critical. By storing hydrogen at an increased density, there is also a flow-on engineering benefit of reduced volume, weight and, hence, cost of the tank needed for storage.[13] It should be noted that the theoretical enthalpy of Reaction 5 is 18.8 kJ/mol H_2. This value is slightly too low for practical applications as it translates to an H_2 equilibrium pressure of ~1515 bar (fugacity of 3280 bar) at 100 °C.

There are two important limitations associated with this predictive method. The first is that it cannot predict the true reaction if the reaction involves a previously unknown compound for which the thermodynamic properties are not known. Secondly, this method gives no information about the kinetics of reactions. Therefore, it may predict a reaction that is not observed experimentally due to kinetic limitations.[9]

Examination of the literature on sulphur-hydrogen compounds reveals a rich history of research into thiols (hydrocarbon – sulphur – hydrogen compounds) and thiolates (metal – sulphur – hydrogen compounds) with the main focus being on catalysis, surface passivation and the fundamentals of self-assembled monolayer formation. These systems show that under the right conditions metal – sulphur – hydrogen systems can reversibly release hydrogen without the need for catalysts.[14, 15]

The thermodynamic predictions of complex hydrides mixed with metal sulphides and the experimental work of hydrogen release from thiols and thiolates suggests that a new class of sulphur based hydrogen storage materials that do not require the addition of catalysts may be viable. The potential of sulphur based materials and their application in hydrogen storage systems is a new approach that has not previously been considered. Here we present the first results on the novel hydrogen storage systems $NaAlH_4$ – Al_2S_3 that show a onset temperature for hydrogen release below 100 °C and partial hydrogen reversibility without the need for catalysts.

Experimental

Synthesis

All handling and storage of chemicals was performed in argon-filled glove-boxes equipped with circulation purifiers. Sample preparation: NaH (95%, Aldrich), $NaAlH_4$ (95%, Aldrich), and Al_2S_3 (98%, Aldrich) were used as received.

Samples of $NaAlH_4$—Al_2S_3 (6:1) and NaH—Al_2S_3 (6:1) for *in-situ* synchrotron powder X-ray diffraction (SR-XRD) were ball milled using a Fritz Pulveritsette 4 planetary ball mill, a tungsten carbide (WC) vial (80 mL) and 10 mm diameter balls in a ball-to-powder (BTP) ratio of 35:1. The total milling time was 20 minutes ball milling 2 minutes of ball milling and 2 minutes of break, repeated 10 times.

Samples of $NaAlH_4$-Al_2S_3 (6:1) for hydrogen absorption measurements were prepared using a PQ-N04 planetary mill (Across International) using a stainless steel vial (100 mL) and stainless steel balls (diameter: 10 mm). $NaAlH_4$ and Al_2S_3 (6:1, 1g) were also cryogenically milled at 77 K using a Spex 6850 freezer mill using a 2 minute milling, 1 minute cooling cycle for a total of 30 minutes of milling. The milling rod speed was set at 10 impacts per second per side. The high impact rate results in high energy milling while the cryogenic conditions prevents decomposition of the sample that can result from high energy ambient milling.

Other than potential contamination from the milling media, no catalysts were added to the system. All further references to the $NaAlH_4$-Al_2S_3 and NaH-Al_2S_3 systems are for those mixed in a 6:1 molar ratio.

Characterisation

In-situ SR-XRD data (λ = 0.9892 Å and 1.1011 Å) were measured at Beamline I711 at the MAX-II synchrotron in the research laboratory MAX-lab, Lund, Sweden with a MAR165 CCD detector system. The samples were mounted in sapphire (Al_2O_3) single crystal tubes (1.09 mm o.d., 0.79 mm i.d.) in an argon filled glovebox using a specially designed sample holder.[16] The *in-situ* SR-XRD measurements were performed for $NaAlH_4$—Al_2S_3 and NaH—Al_2S_3 heated from room temperature (RT) to 500 °C (5 °C/min) under dynamic vacuum.

Ex-situ SR-XRD data was collected from a sample sealed in a borosilicate capillary (0.3 mm o.d.) at the Australian Synchrotron, Melbourne, Australia (λ = 1.000 Å) with a Mythen microstrip detector.

Laboratory-based XRD patterns of hydrogen cycled $NaIH_4$-Al_2S_3 were performed using a Bruker D8 Advance diffractometer (λ = 1.5406 Å) with a 2θ range of 10 to 70°. The samples were loaded into an XRD sample holder and sealed with a poly(methylmethacrylate) (PMMA) airtight bubble within a glovebox to prevent oxygen/moisture contamination during data collection. The PMMA airtight bubble results in broad humps in XRD patterns centred at 10° and 20° 2θ, respectively. Quantitative analysis of one unknown phase was achieved by using an internal standard to calibrate a PONKCS (Partial Or No Known Crystal Structure) phase.[17] This method substitutes a crystal structure for a set of peaks (or a Le Bail fit) associated with an unknown phase that may be scaled in unison similar to the set of structure factors derived from a crystal structure. Once the PONKCS phase is calibrated with an internal standard, it can

be used for quantitative phase analysis. Rietveld refinement and unit cell indexing was performed using version 4.2 of the TOPAS software (Bruker-AXS).

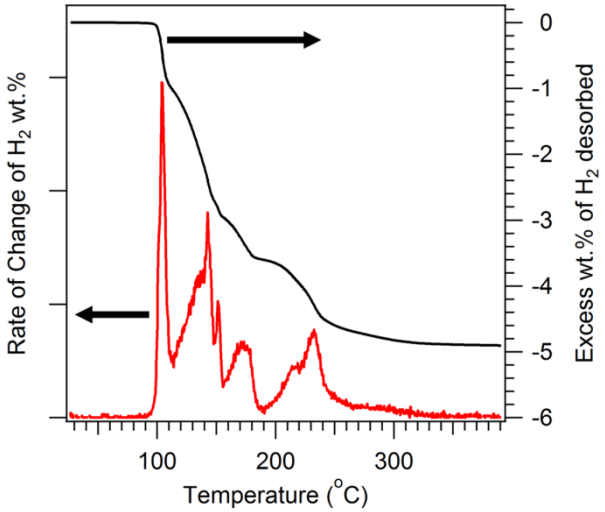

Fig 2. Temperature Programmed Desorption (TPD-MS) of $NaAlH_4$-Al_2S_3 ball-milled for 6 h. Heating rate = 1 ^{o}C/min.

Fourier transform infrared spectroscopy (FTIR) spectra were collected using a Bruker IFS 66 FT-IR with 64 background and 64 sample scans. The spectrometer was purged with dry nitrogen and samples were prepared by encapsulation within pressed KBr pellets.

Temperature Programmed Desorption Mass Spectrometry (TPD-MS) on $NaAlH_4$-Al_2S_3 was performed on a PCT-Pro E&E (Hy-Energy) coupled to a quadrupole mass spectrometer residual gas analyser (Stanford Research Systems RGA 300) that monitored from 1 to 58 atomic mass units (AMU). For each measurement, approximately 30 mg of sample was outgassed at 3 x 10^{-7} bar and 25 ^{o}C overnight. While still under vacuum, the samples were heated up to 375 ^{o}C at a heating rate of 1 ^{o}C/min.

Ex-situ XRD and FTIR patterns were collected on the $NaAlH_4$-Al_2S_3 system, where repeat TPD-MS measurements were halted at 115, 150, 160, 195, 275 and 375 ^{o}C, and then cooled quickly to room temperature. These samples shall be referred to as TPD-115, TPD-150, TPD-160, TPD-195, TPD-275 and TPD-375, respectively.

The H_2 release and uptake for $NaAlH_4$-Al_2S_3 were measured on two separate custom-made Sieverts/volumetric instruments. Both instruments utilized Rosemount pressure transducers (Model 3051S) with an accuracy of 0.01% of their maximum pressure (150 and 690 bar, respectively). Initially, samples of $NaAlH_4$-Al_2S_3 were evacuated at room temperature and then desorbed of H_2 by heating to 380 ^{o}C at 11 ^{o}C/min under either their evolved hydrogen pressure (to confirm wt.% of H_2 desorbed) or vacuum. Absorption measurements were performed by loading a known reference volume to the target pressure and then opening it to the sample volume. The absorption pressures quoted in the text are the final pressures the system reached after absorption was complete.

Safety warning: Handling of these samples comprises a number of safety hazards. $NaAlH_4$ reacts violently with water and may spontaneously combust in air. Exposure of Al_2S_3 (and metal sulphides in general) to water or atmospheric moisture releases toxic H_2S gas.

Results

TPD-MS on $NaAlH_4$-Al_2S_3 (6:1)

TPD-MS up to 390 ^{o}C of $NaAlH_4$-Al_2S_3 milled for 6 h (Figure 2) showed multiple H_2 release events below 300 ^{o}C, with the first small release beginning below ~100 ^{o}C. The sample released a total of 4.91 wt.% of H_2 in good agreement with the theoretically predicted value of 5.1 wt.%. Given the presence of sulphur in these samples, the potential release of H_2S or other sulphanes is of concern due to their toxicity. Additionally, the formation and loss of H_2S from the system would reduce the cyclic H_2 capacity. However, TPD-MS showed that only H_2 was released for all samples when adequately outgassed prior to measurement. Insufficient degassing resulted in H_2, H_2O and H_2S release below 100 ^{o}C due to the reaction between atmospheric moisture physisorbed on the sample cell and the sample. The multiple H_2 release events observed in Figure 2 are in contrast to the single decomposition step predicted by the thermodynamic software HSC.[12] The discrepancy is not entirely unexpected, however, as the software can only predict reaction pathways including known phases, and does not include any kinetic considerations.

XRD of the product after decomposition to 390 °C, Figure S1, showed only the expected decomposition products of Na_2S and Al (see Reaction 5). One possible explanation for detecting multiple desorption events is hindered kinetics in parts of the sample due to insufficient milling.[18] This could be a result of inadequate mixing of the starting reagents due to the large volume difference between them ($NaAlH_4$ = 77 vol.%, Al_2S_3 = 23 vol.%). To explore this hypothesis further, several $NaAlH_4$-Al_2S_3 samples were synthesized with different milling times and BTP ratios. Decreasing the milling time to 3 h (BTP = 15:1), Figure S2 (a), again resulted in multiple H_2 release events. However, in this case, the temperatures and relative intensities of the desorption events are distinctly different. This suggests that decomposition of the $NaAlH_4$-Al_2S_3 system involves competing kinetic and thermodynamic pathways. In other complex hydride systems, the kinetics are known to be controlled by bulk diffusion rates.[19, 20] However, in the $NaAlH_4$-Al_2S_3 system the change in diffusion length is responsible for the improved kinetics as the bulk diffusion rates can only be changed by altering the chemical composition of the sample.[19]

Increasing the milling time to 15 h (BTP = 90:1) resulted in the loss of the first hydrogen release event, Figure S2 (c), and XRD after milling showed the presence of ~3.5 wt.% Al that was absent in samples milled for shorter durations. This result shows that prolonged energetic milling resulted in partial decomposition of the starting reagents. The remaining hydrogen desorption events were similar to the sample ball milled for 6 h and the cryo-milled sample, Figure S2 (d). These results suggest that the multiple hydrogen desorption events observed are due to the formation and decomposition of intermediate phases that were not predicted in the initial thermodynamic calculations.

In-situ SR-XRD of $NaAlH_4$-Al_2S_3

To gain further insight into the multiple decomposition pathways, *in-situ* synchrotron XRD was performed on $NaAlH_4$-Al_2S_3 during

decomposition under vacuum at a heating rate of 5 °C/min (Figure 3(a)). The decomposition pathway is complex, with multiple phase transformations (mirroring the TPD-MS results), and the formation of an array of as-yet unknown phases. At 132 °C reflections from $NaAlH_4$ and Al_2S_3 begin to decrease in intensity and three new compounds form: Al and two unidentified phases that we have designated α and β respectively. The α – phase has only very low intensity peaks, begins to decompose at

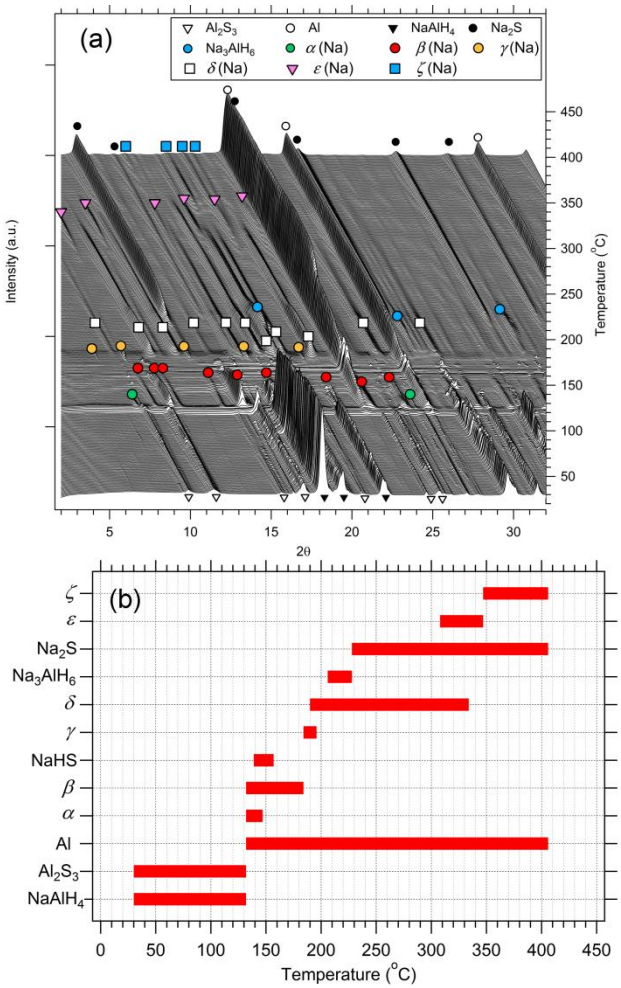

Fig 3. (a) *In-situ* SR-XRD of $NaAlH_4$-Al_2S_3 decomposed under vacuum at a heating rate of 5 °C/min, λ = 0.9892 Å and (b) a summary of the stable temperature ranges for the phases observed during decomposition.

139 °C and is associated with the formation of an XRD peak at $2\theta \sim 18.6°$ (this peak is obscured by the intense $NaAlH_4$ peaks in Figure 3 (a)). This peak corresponds to the high-temperature cubic phase of NaHS that is stable above ~92 °C.[21] However, the quality of the data and the high degree of peak overlap with other phases makes this assignment tentative. The NaHS peak continues to grow until the α – phase disappears at 147 °C. The β - phase and NaHS begin to decompose at 150 °C with NaHS completely decomposed by 157 °C. The β - phase continues to slowly decrease in intensity and disappears by 184 °C where peaks from γ begin to form. The γ - phase is short-lived and is gone by 196 °C. At 190 °C, reflections from yet another unknown phase, δ, form and reflections from Na_3AlH_6 also begin to form at 206 °C. The formation of Na_2S begins at 228 °C and coincides with the disappearance of Na_3AlH_6, a decrease in the intensity of the δ - phase and an increase in the intensity of Al. The remaining δ phase peaks remain stable up to 308 °C where weak reflections from an unknown phase, ε, appear. This conversion to the ε - phase is quite slow and the last reflections from the δ – phase finally disappear at 334 °C. At 347 °C reflections from the ε - phase decrease in intensity and weak reflections from another unknown ζ - phase appear. The reflections from Na_2S, Al and the ζ - phase are stable up until the experiment ends at 406 °C. Given the complexity of the decomposition pathway, a summary of the phases and the temperature range over which they are stable is shown in Figure 3(b). With the possible exception of the α – phase, none of the unknown phases match any known Na/Al/S/O/H compounds. The α – phase may match NaOH but the low intensity of the peaks and the large number of overlapping peaks makes definitive determination difficult.

As a comparison, *in-situ* SR-XRD was also performed on NaH-Al_2S_3 (Figure S3). This reaction is predicted to be exothermic (ΔH = -37.7 kJ/mol.H_2)[12] but *in-situ* SR-XRD should reveal if the unknown phases observed in the decomposition of $NaAlH_4$-Al_2S_3 are due to the interaction between $NaAlH_4$ and Al_2S_3 or the interaction between NaH and Al_2S_3 after $NaAlH_4$ has begun to decompose. Figure S3 reveals that NaH begins to react with Al_2S_3 at 195 °C in a single-step reaction with the direct formation of Na_2S and Al according to reaction 6:

$$6NaH + Al_2S_3 \rightarrow 3Na_2S + 2Al + 3H_2 \quad \text{Reaction 6}$$

This indicates that the unknown phases seen during *in-situ* SR-XRD of $NaAlH_4$-Al_2S_3 are in-fact due to alternate chemical reactions from the complex sulphur chemistry, where a range of different compounds may be formed as intermediates.

Ex-situ FTIR and XRD on $NaAlH_4$-Al_2S_3

Ex-situ XRD after TPD to 115 °C (TPD-115), Figure 4 (a)(i), only shows the presence of $NaAlH_4$ and Al. All traces of Al_2S_3 have disappeared and no other sulphur containing compounds are present, suggesting that all of the sulphur is bound within amorphous or nanocrystalline phases. No other sodium containing compounds are evident, which suggests that all of the sodium from $NaAlH_4$ decomposition is present in the amorphous or nanocrystalline sulphur containing compound. Rietveld refinement reveals that $NaAlH_4$ comprises ~78 wt.% of the crystalline portion of the sample and Al ~22 wt.%. The 1.0 wt.% of H_2 lost in this temperature range is insufficient to account for the mass ratio of $NaAlH_4$ and Al in the crystalline products. This suggests that either some of the crystalline Al comes from Al_2S_3 or that there is some hydrogen remaining in the amorphous/nanocrystalline phase. *Ex-situ* FTIR, Figure 4 (b)(i), shows that, after TPD at 115 °C, absorption bands associated with $NaAlH_4$ at 1678, 900, 740 and the shoulder at ~660 cm^{-1} are still present [22] and that the three bands at 503, 459 and 422 cm^{-1} associated with pure Al_2S_3 (Figure S4 (a)) have disappeared. In their place is a broad absorption band extending from 480 cm^{-1} to 400 cm^{-1} and centered at 424 cm^{-1}. No other changes occur in the FTIR pattern that can be associated with the amorphous or nanocrystalline sulphur containing phase. For comparison, FTIR of pure $NaAlH_4$ (Figure S4 (b)) and 6 h ball-milled $NaAlH_4$-Al_2S_3 (Figure S4(c)) are also included.

Ex-situ XRD on TPD-150, Figure 4 (a)(ii), shows $NaAlH_4$, Al and the δ - phase. The room-temperature rhombohedral polymorph of NaHS was also indentified.[19] Using the PONKCS (Partial Or No Known Crystal Structure) method, [17] as outlined in the Experimental Characterisation section, quantitative phase analysis yielded $NaAlH_4$ ~ 10 wt.%, NaHS ~ 7 wt.%, Al ~ 20 wt.% and the δ - phase ~ 63 wt.%. *Ex-situ* FTIR, Figure 4 (b)(ii), shows a pronounced decrease in the intensity of the main $NaAlH_4$ bands and the formation of a shoulder at ~1606 cm^{-1}. Bands also formed at ~823, 690, 571,

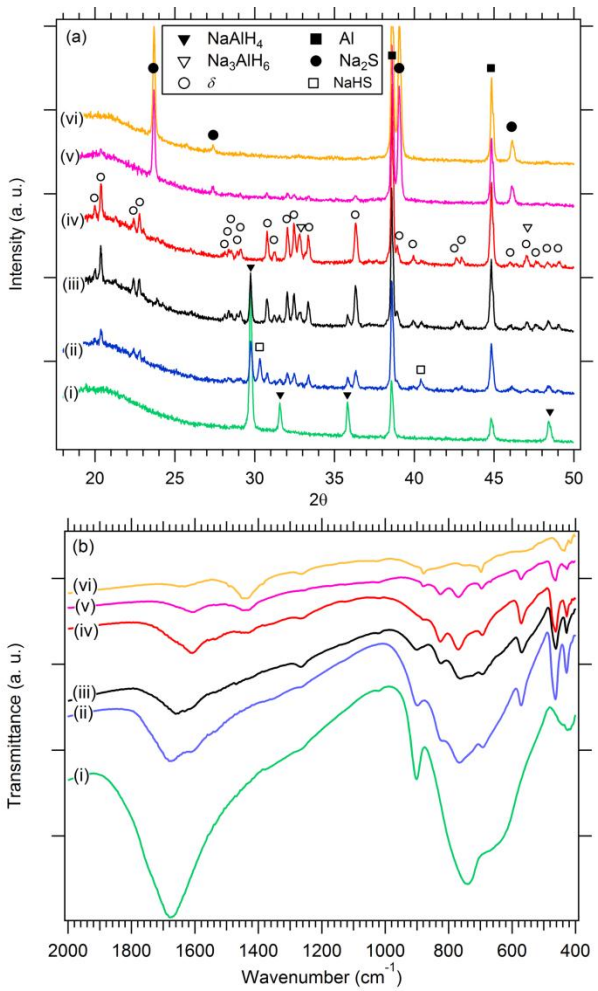

Fig 4. (a) *Ex-situ* XRD (λ = 1.5406 Å) of $NaAlH_4$-Al_2S_3 decomposed under vacuum at a heating rate of 1 °C/min up to (i) 115 °C, (ii) 150 °C, (iii) 165 °C, (iv) 195 °C, (v) 275 °C and (vi) 375 °C. (b) The corresponding *ex-situ* FTIR of $NaAlH_4$-Al_2S_3 decomposed under vacuum at a heating rate of 1 °C/min up to (i) 115 °C, (ii) 150 °C, (iii) 165 °C, (iv) 195 °C, (v) 275 °C and (vi) 375 °C.

463 and 428 cm^{-1}. NaHS identified by *ex-situ* XRD in trace levels and *ex-situ* FTIR cannot resolve the typical NaHS FTIR active modes at 2544, 1850 and ~450 cm^{-1}.[23] So we can attribute the new bands in the FTIR pattern to the only other compound present, δ - phase.

Ex-situ XRD on TPD-160, Figure 4 (a)(iii), shows that the NaHS phase has disappeared, also shows a decrease in $NaAlH_4$ content to 4.1 wt.%, the appearance of Na_3AlH_6 (1.5 wt.%), a decrease in Al content to 14.2 wt.% and an increase in the $\delta-$ phase to 80.2 wt.%. The decomposition of NaHS between 150 and 160 °C is somewhat unexpected given that the melting point of NaHS is 350 °C.[24] The *ex-situ* FTIR, Figure 4 (b)(iii) is similar to the previous pattern but with a slight enhancement of the shoulder at 1606 cm^{-1} at the expense of the $NaAlH_4$ peak at 1678 cm^{-1}. This represents a decrease in the stretching vibrations of AlH_4^{-1}. This shift is not related to the formation of Na_3AlH_6 or the AlH_6^{-3} anion, as the main band for Na_3AlH_6 at 1275 - 1300 cm^{-1} is absent.[22,25] A similarly small decrease in the frequency of AlH_4^{-1} stretching vibrations has been seen during the decomposition of $KAlH_4$, [26] which was attributed to an increase in co-ordination number about the Al atom and the formation of K_yAlH_x ($y \geq 1$ and $x > 4$). However it should be noted that relatively small structural changes in the local environment of the AlH_4^{-1} anion can also cause shifts in the position of the stretching band at 1675 cm^{-1}.[20]

Ex-situ XRD on TPD-195, Figure 4 (a)(iv) shows the complete disappearance of $NaAlH_4$ and an increase in Na_3AlH_6 to ~ 4.6 wt.%, a slight decrease in Al (17.8 wt.%) and a slight decrease in the $\delta-$ phase (77.6 wt.%). The associated *ex-situ* FTIR, Figure 4 (b)(iv) clearly shows the band at 1606 cm^{-1} has been growing and reveals that bands associated with $NaAlH_4$ are absent. A band has also begun to form at ~1440 cm^{-1}. The bands below 600 cm^{-1} remain unchanged while the bands at 827, 767 and 692 cm^{-1} become more clearly resolved.

Ex-situ XRD on TPD-275, Figure 4 (a)(v), shows the formation of Na_2S (~38.1 wt.%), an increase in Al (~ 38.4 wt.%) and a decrease in the $\delta-$ phase (~23.5 wt.%). FTIR, Figure 4 (b)(v), shows that the band at 1440 cm^{-1} has increased in intensity relative to all other bands and that the band at 1606 cm^{-1} has decreased in intensity.

Ex-situ XRD of TPD-375, Figure 4 (a)(vi), shows complete removal of the δ - phase. FTIR, Figure 4 (b)(vi), shows further enhancement of the band at 1440 cm^{-1} at the expense of the δ - phase band at 1606 cm^{-1}. Bands associated at 827 cm^{-1}, 769 cm^{-1}, 571 cm^{-1}, 463 cm^{-1} and 426 cm^{-1} have disappeared, whilst the bands at 879 cm^{-1} and 698 cm^{-1} have remained. In addition, the three bands below 500 cm^{-1} have transformed into a single band at 436 cm^{-1}. FTIR performed on pure Na_2S (Figure S4 (d)) revealed that only the band at 1440 cm^{-1} can unambiguously be attributed to Na_2S. As a result, the other bands present after decomposition cannot be ruled out as being due to minor impurity phases such as oxides.

Based on TPD-MS and the *ex-situ* XRD and FTIR measurements, some conclusions can be drawn about the nature of the $\delta-$ phase: (1) The $\delta-$ phase contains hydrogen and; (2) the hydrogen is coordinated to Al, probably as AlH_4^{-1}, rather than bound to S as a hydrosulphide ion, SH^{-1}. *In-situ* SR-XRD and *ex-situ* XRD also provide some interesting insights into the role of NaHS in the system. There are some discrepancies in the decomposition observed via *in-situ* SR-XRD compared to *ex-situ* XRD. The primary differences are that the formation of the $\delta-$ phase and the formation of Na_3AlH_6 occur ~30-40 °C lower in temperature in the *ex-situ* XRD measurements compared to *in-situ* SR-XRD. This difference can readily be explained by the difference in heating rate used in the *ex-situ* XRD measurements (1 °C/min) and the *in-situ* SR-XRD measurements (5 °C/min). However, the narrow temperature range for the formation and decomposition of NaHS is near identical for both sets of measurements. Combined

with the fact that NaHS disappears well below its melting point suggests that it is undergoing decomposition via a chemical reaction with a very low activation energy and rapid kinetics. However, further experimental work is needed to verify this.

Hydriding Properties of $NaAlH_4$-Al_2S_3

Hydrogen absorption was attempted after decomposing $NaAlH_4$-Al_2S_3 under vacuum whilst ramping to 375 °C. Initial re-hydrogenation at 125 °C under a H_2 pressure of 85 bar yielded 1.36 wt.% H_2 absorption but required 24 h to reach this value. Subsequent re-hydrogenation, using the same sample, at 200 °C, Figure 5 (a), revealed the hydrogen absorption capacity and rate

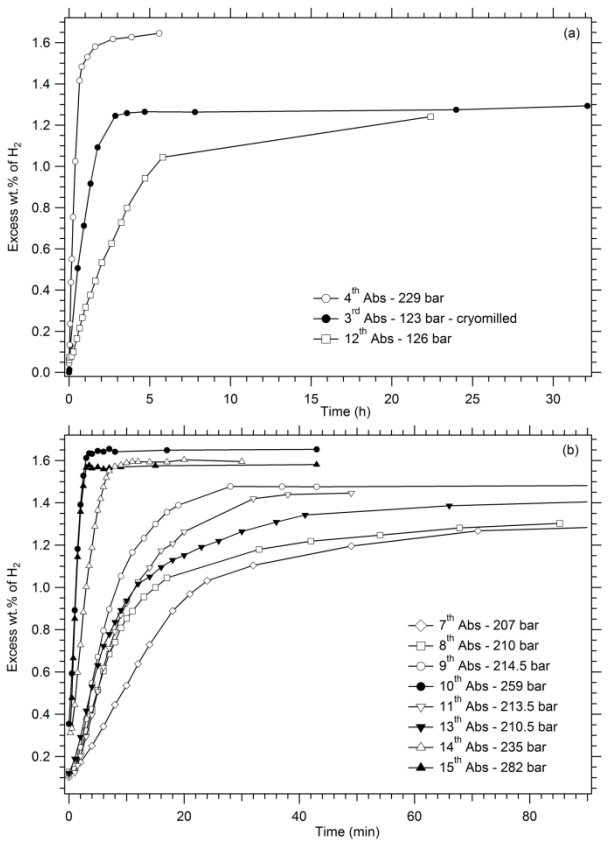

Fig 5. (a) Hydrogen absorption at 200 °C on $NaAlH_4$-Al_2S_3 milled for 6 h or cryomilled for 30 minutes. (b) Hydrogen absorption at 300 °C on $NaAlH_4$-Al_2S_3 milled for 6 h.

to be dependent on the milling method, the applied hydrogen pressure and cycle number. Under an applied hydrogen pressure of 123 - 126 bar, $NaAlH_4$-Al_2S_3 cryomilled for 30 minutes or ball-milled for 6 h both absorbed comparable amounts of hydrogen but at different rates. $NaAlH_4$-Al_2S_3 cryomilled for 30 minutes absorbed 1.25 wt.% of H_2 in 3 h and then slowly absorbed up to 1.36 wt.% over the next 48 h. In contrast, $NaAlH_4$-Al_2S_3 ball-milled for 6 h only reaches 1.05 wt.% of H_2 absorption after 6 h and reaches 1.25 wt.% after 24 h absorption. An increased H_2 pressure, 229 bar, resulted in both an increased H_2 uptake and absorption rate. In this case, H_2 absorption reached 1.50 wt.% within 1 h and reached 1.65 wt.% in 6 h. This increased capacity suggests that the absorption measurements at lower pressure had either not reached completion due to kinetic restrictions or that a second absorption step (requiring higher pressure) occurred between 1.36 wt.% and 1.65 wt.% of H_2. In order to assess these possibilities, absorption was subsequently performed, on the same sample, at 300 °C where the kinetics should be improved. Figure 5 (b) shows the hydrogen kinetics and hydrogen uptake as a function of time, applied hydrogen pressure and absorption cycle. With an applied hydrogen pressure of between 207 and 214.5 bar, the hydrogen uptake varied between 1.39 and 1.47 wt.%, respectively, and the time required to reach these values varied between 30 minutes and 15 h. Increasing the applied pressure to 235 bar resulted in near full absorption in ~10 minutes while increasing the pressure further still to 259 bar or above reduced this time to 3 - 4 minutes.

The high temperature, 300 °C, combined with the destabilization of the system, relative to pure $NaAlH_4$, necessitates high H_2 pressures for reabsorption (a minimum H_2 pressure of 204 bar at 300 °C was required to initiate absorption). The system reaches absorption equilibrium in 3 - 4 minutes when the applied H_2 pressure is greater than 259 bar at 300 °C and suggests that insufficient H_2 pressure is the limiting factor to promote hydrogenation rather than kinetics. To test this theory, experiments need to be performed under higher pressure at 300 °C or the kinetics need to be improved at lower temperatures.

Hydrogen desorption at 300 °C was performed against a hydrogen back pressure between 63 and 76 bar, Figure S5. In all cases, desorption is exceedingly fast with hydrogen release essentially complete within 2 minutes. This demonstrates that there are clearly two different kinetic mechanisms controlling the absorption and desorption processes.

Ex-situ SR-XRD (Figure S6) was performed on the sample hydrided at 300 °C under 282 bar H_2 pressure (absorption cycle number 15 from Figure 5(b)) and revealed the major phases to be Al, $NaAlH_4$ and the $\delta-$ phase. A minor amount of NaHS and residual Na_2S was also observed. From Figure S6 the δ - phase was successfully indexed as monoclinic (possible space group of P2 or P21) with unit cell parameters of a = 9.680 ± 0.007 Å, b = 6.829 ± 0.007 Å, c = 9.489 ± 0.007 Å, β = 67.44 ± 0.05° and a unit cell volume of 579 Å.

Conclusions

The addition of Al_2S_3 acts to effectively thermodynamically destabilize sodium aluminium hydride. The decomposition occurs via complex reaction pathways with numerous, as-yet, unknown intermediate phases.

Hydrogen desorption is kinetically limited at low temperature but hydrogen can be released at temperatures lower than 100 °C for $NaAlH_4$-Al_2S_3. Hydrogen absorption requires high temperatures (200 °C – 300 °C) and, consequently, high pressures to overcome slow absorption kinetics. A stable reversible hydrogen capacity of 1.65 wt% was measured at 300 °C. The potential for higher hydrogen absorption requires either improving the kinetics at lower temperatures so that lower pressures can be used or higher hydrogen pressure at 300 °C.

The multitude of unknown phases that exist in this system warrants isolation and further investigation. These phases may be viable as hydrogen storage materials in their own right or as components in reactive hydride composites. The use of sulphur-containing compounds as thermodynamic destabilizing agents is a novel method for hydrogen storage that now opens up a

research avenue to study a range of other complex hydride systems with sulphur-based destabilization agents.

Acknowledgements

C.E.B, D.A.S and M.P acknowledge the financial support of the Australian Research Council (ARC) for ARC Linkage grant LP120101848 C.E.B, D.A.S and M.P also acknowledge that part of this research was undertaken on the Power Diffraction beamline at the Australian Synchrotron, Victoria, Australia. C.E.B. also acknowledges ARC LIEF grants LE0775551 and LE0989180, which enabled the XRD and gas sorption studies to be done. The Danish Strategic Research Council is acknowledged for financial support the project HyFillFast, while the Danish National Research Foundation is thanked for funding to the Center for Materials Crystallography. Finally, we are thankful to MAX-lab for the provision of beam time.

Notes and references

[a] *Department of Imaging and Applied Physics, Fuels and Energy Technology Institute, Curtin University, GPO Box U1987, Perth 6845, WA, Australia. Fax: 61 8 9266 2377; Tel: 61 8 9266 1381; E-mail: drew.sheppard@gmail.com*

[b] *Interdisciplinary Nanoscience Center (iNANO) and Department of Chemistry, University of Aarhus, DK-8000, Denmark.*

† Electronic Supplementary Information (ESI) available: Additional XRD, *in-situ* and *ex-situ* SR-XRD, FTIR, TPD and hydrogen desorption kinetic data. See DOI: 10.1039/b000000x/

1. D. Abbott, *Proceedings of the IEEE*, 2010, **98**, 24.
2. L. H. Rude, T. K. Nielsen, D. B. Ravnsbæk, U. Bösenberg, M. B. Ley, B. Richter, L. M. Arnbjerg, M. Dornheim, Y. Filinchuk, F. Besenbacher and T. R. Jensen, *Physica Status Solidi A*, 2011, **208**, 1754-1773.
3. B. Bogdanović and M. Schwickardi, *Journal of Alloys and Compounds*, 1997, **253-254**, 1-9.
4. B. C. Hauback, *Zeitschrift für Kristallographie*, 2008, **223**, 636-648.
5. M. P. Pitt, P. E. Vullum, M. H. Sørby, H. Emerich, M. Paskevicius, C. E. Buckley, J. C. Walmsley, R. Holmestad and B. C. Hauback, *The Journal of Physical Chemistry C*, 2012, **116**, 14205-14217.
6. M. P. Pitt, P. E. Vullum, M. H. Sorby, D. Blanchard, M. P. Sulic, H. Emerich, M. Paskevicius, C. E. Buckley, J. C. Walmsley, R. Holmestad and B. C. Hauback, *Journal of Alloys and Compounds*, 2012, **513**, 597-605.
7. J. M. Bellosta von Colbe, O. Metz, G. A. Lozano, P. K. Pranzas, H. W. Schmitz, F. Beckmann, A. Schreyer, T. Klassen and M. Dornheim, *International Journal of Hydrogen Energy*, 2012, **37**, 2807-2811.
8. M. P. Pitt, P. E. Vullum, M. H. Sørby, H. Emerich, M. Paskevicius, C. J. Webb, E. M. Gray, C. E. Buckley, J. C. Walmsley, R. Holmestad and B. C. Hauback, *International Journal of Hydrogen Energy*, 2012, **37**, 15175-15186.
9. S. V. Alapati, Johnson, J. K., Sholl, D. S., *Journal of Physcal Chemistry C*, 2008, **112**, 5258 - 5262.
10. B. Bogdanović, R. A. Brand, A. Marjanović, M. Schwickardi and J. Tölle, *Journal of Alloys and Compounds*, 2000, **302**, 36-58.
11. B.-M. Lee, J.-W. Jang, J.-H. Shim, Y. W. Cho and B.-J. Lee, *Journal of Alloys and Compounds*, 2006, **424**, 370-375.
12. HSC Chemistry, Outotech Research Oy, 2007.
13. G. A. Lozano, C. N. Ranong, J. M. Bellosta von Colbe, R. Bormann, J. Hapke, G. Fieg, T. Klassen and M. Dornheim, *International Journal of Hydrogen Energy*, 2012, **37**, 2825-2834.
14. A. Ulman, *Chemical Reviews*, 1996, **96**, 1533-1554.
15. O. Voznyy and J. J. Dubowski, *The Journal of Physical Chemistry C*, 2008, **112**, 3726-3733.
16. T. R. Jensen, T. K. Nielsen, Y. Filinchuk, J.-E. Jørgensen, Y. Cerenius, E. M. Gray and C. J. Webb, *Journal of Applied Crystallography*, 2010, **43**, 1456-1463.
17. N. V. Y. Scarlett and I. C. Madsen, *Powder Diffraction*, 2006, **21**, 278-284.
18. M. P. Pitt, M. Paskevicius, C. J. Webb, D. A. Sheppard, C. E. Buckley and E. M. Gray, *International Journal of Hydrogen Energy*, 2012, **37**, 4227-4237.
19. P. A. Anderson, P. A. Chater, D. R. Hewett and P. R. Slater, *Faraday Discussions*, 2011, **151**, 271-284.
20. A. Borgschulte, M. O. Jones, E. Callini, B. Probst, S. Kato, A. Züttel, W. I. F. David and S.-i. Orimo, *Energy & Environmental Science*, 2012, **5**, 6823-6832.
21. F. Haarmann, H. Jacobs and W. Kockelmann, *The Journal of Chemical Physics*, 2000, **113**, 6788-6794.
22. S. Gomes, G. Renaudin, H. Hagemann, K. Yvon, M. P. Sulic and C. M. Jensen, *Journal of Alloys and Compounds*, 2005, **390**, 305-313.
23. K. Beckenkamp, H. D. Lutz, H. Jacobs and U. Metzner, *Journal of Solid State Chemistry*, 1994, **109**, 241-250.
24. R. E. Eibeck and B. D. James, *Inorganic Syntheses*, 1963, **7**, 128-131.
25. E. C. Ashby and B. D. James, *Inorganic Chemistry*, 1969, **8**, 2468-2472.
26. J. R. Ares, K.-F. Aguey-Zinsou, F. Leardini, I. J. m. Ferrer, J.-F. Fernandez, Z.-X. Guo and C. Sánchez, *The Journal of Physical Chemistry C*, 2009, **113**, 6845-6851.